

Article

# Polyaniline Nanoparticles: A Novel Additive for Augmenting Thermal Conductivity and Tribo-Properties of Mineral Oil and Commercial Engine Oil

Vinay Saini \* and Jayashree Bijwe \*

Centre for Automotive Research &amp; Tribology (CART), Formerly (ITMMEC), Indian Institute of Technology Delhi, Delhi 110016, India

\* Correspondence: vinaysaini.8721@gmail.com (V.S.); jbijwe@gmail.com (J.B.)

**Abstract:** The present work demonstrates the novel composition of nanoparticles (NPs) of polyaniline (PANI) solo and, in combination with particles of polytetrafluoroethylene (PTFE) ~230 nm, as a powerful additive (antiwear-AWA and extreme-pressure additive EPA) in lubricating oils. The concentration of PANI NPs varied from 1–4 wt.% in a base oil and commercial 5W30 engine oil. The tribo-performance was evaluated on a four-ball tester. The PANI-based oils significantly enhanced the load-bearing ability, and 3 wt.% of PANI NPs led to enhancement in EP properties by 220% in a base oil and 58% in engine oil. Additionally, hybrid combinations of NPs of PTFE with PANI in base oil were prepared by mixing in a ratio of 3:1 and 2:1 and were explored for possible tribo-synergism in EP properties. The hybrid nano-oils led to the highest reported ~ 535% enhancement in the load-carrying capacity of mineral oil. The lubrication mechanisms for enhanced tribo performance were linked with studies on a scanning electron microscope, an energy-dispersive X-ray analyzer, and with the use of Raman spectroscopy.

**Keywords:** polyaniline (PANI) nanoparticles; polytetrafluoroethylene; weld load; synergism; nano-oils; anti-wear additive



Citation: Saini, V.; Bijwe, J.

Polyaniline Nanoparticles: A Novel Additive for Augmenting Thermal Conductivity and Tribo-Properties of Mineral Oil and Commercial Engine Oil. *Lubricants* **2022**, *10*, 300.<https://doi.org/10.3390/lubricants10110300>

Received: 17 October 2022

Accepted: 5 November 2022

Published: 9 November 2022

**Publisher's Note:** MDPI stays neutral with regard to jurisdictional claims in published maps and institutional affiliations.



**Copyright:** © 2022 by the authors. Licensee MDPI, Basel, Switzerland. This article is an open access article distributed under the terms and conditions of the Creative Commons Attribution (CC BY) license (<https://creativecommons.org/licenses/by/4.0/>).

## 1. Introduction

Modern machines operate at higher contact pressures due to downsizing and other complex technologies, increasing friction and wear at contact interfaces. High friction generates excessive heat at the tribo-interface, which shortens component life. Also, to comply with the most recent automotive environmental legislation, automotive companies are pushing for low-viscosity lubricants with low SAPs (sulfur and phosphate ash). Lubricants with low viscosity improve the fuel efficiency of engines and other machines by reducing the viscous drag forces. However, lubricants with lower viscosity are more prone to higher wear. Lower viscosity results in a thinner oil film, which forces the surface in contact to operate in the boundary lubrication regime, resulting in increased wear. This ultimately reduces the durability and lifespan of the equipment's moving components. Therefore, research on new additives to address these issues is most urgent. Effective lubrication of tribo-components with novel eco-friendly tribo additives is urgently required to reduce frictional energy and thereby increase component life. Therefore, scientists have been exploring various options for cost-effective, green, renewable [1], eco-friendly [2,3] solutions and additives for water [4], oils [5,6], and greases. As potential substitute additives, the scientific community has investigated various types of NPs. The NPs have great potential due to exceptional inherent properties such as high surface area, high potential for reactivity (physical or chemical), and chemical affinity. Moreover, owing to their tiny size, the NPs can operate by entering the tribo-contacts zone and provide better film-forming than micron-sized (MPs) particles.

The oils formulated using NPs as additives are generally referred to as nano lubricants [7] and nano oils. Over a period, several types of NPs based on different morphology, sizes, amounts, and combinations [8–10] have been reported as lubricious additives across a broad array of lubricating oils [11–15] and greases [16–18] based on various lubrication mechanisms (Rolling, Mending, protective film, Polishing) [19–21]. According to the literature, Polymer-based PTFE (230 nm) NPs have shown the highest ability to enhance extreme-pressure (EP) performance by ~454% [14], offering a significant advantage if operating at higher loads. Whereas lamellar-based NPs and flakes of MoS<sub>2</sub> [22], Talc [23–25], and Graphene [26–28] with the larger surface area have shown better antiwear (AW) properties at lower loads. Due to strong in-plane but relatively weak out-of-plane bonding in two-dimensional (2D) materials, single nanosheets get exfoliated under applied shear stress from their respective bulk crystals. These exfoliated nanosheets have few atomic layers in terms of thickness. Still, they can be micrometres wide depending on the size of 2D nanomaterials and act as an interfacial film between sliding contacts. In a broader perspective, the lubrication performance of NPs as additives is conditional to various factors such as base oils [12,29], sizes of NPs [10,30], shapes [10,27], concentration, and combinations with other NPs, and dispersants employed during formulation. However, along with tribo-properties, many lube manufacturers are working to enhance the thermal conductivity of oils to prevent the oil from thermal degradation.

In literature other than NPs, different Ionic Liquids (ILs) have been explored for their potential as lubricating additives, mainly owing to their ionic nature that promotes their adsorption on metallic surfaces [31–33]. Combinations of NPs-ILs are also researched as hybrid nanolubricants (NLs) [34–36]. The interaction of hBN, ZnO NPs was studied explicitly with three different ILs, namely, trihexyltetradecylphosphonium bis(2,4,4-trimethylpentyl) phosphinate (BTMPP), trihexyltetradecylphosphonium bis(2-ethylhexyl) phosphate (DEHP) and trihexyltetradecylphosphonium dibutyl phosphate (DBP) in PAO6 as a base oil [15]. The authors reported a significant reduction in friction (23–30%) and wear (41–57%) for DEHP and DBP-based hybrid NLs [15]. The lubrication mechanisms were linked to the formation of Iron phosphate (FePO<sub>4</sub>) rich tribo-film with tribo-sintered NPs. However, as EPA these hybrid oils could sustain a load of only 175 kg. Moreover, the ILs are very expensive and have limited applicability for phosphonium-based ILs due to the presence of phosphorus (P), which is not eco-friendly

Polyaniline (PANI) is an eco-friendly conductive organic polymer synthesized from low-cost aniline as a monomer (the chemical formula and structure are shown in Figure 1a). PANI is a conducting polymer commercially available in dark blue-green color as NPs. The potential of PANI NPs has already been successfully explored as a replacement for copper in non-asbestos organic brake-pad formulations [37]. However, its potential as an oil-additive remains unexplored. The present work explores the potential of NPs of PANI as AWA and EPA, in mineral oil and also commercial oil, which is already packaged with very efficient AWA/EWA. To work in tandem with existing oil additives is the most challenging. Two series of PANI-nano-oils were developed by varying their concentration (1–4 wt.%) and using mineral oil and engine oil. Furthermore, based on previously reported work on PTFE NPs in oils, two-hybrid oils were also developed using both NPs to explore the synergism, if any, and details of the work are discussed in subsequent sections.

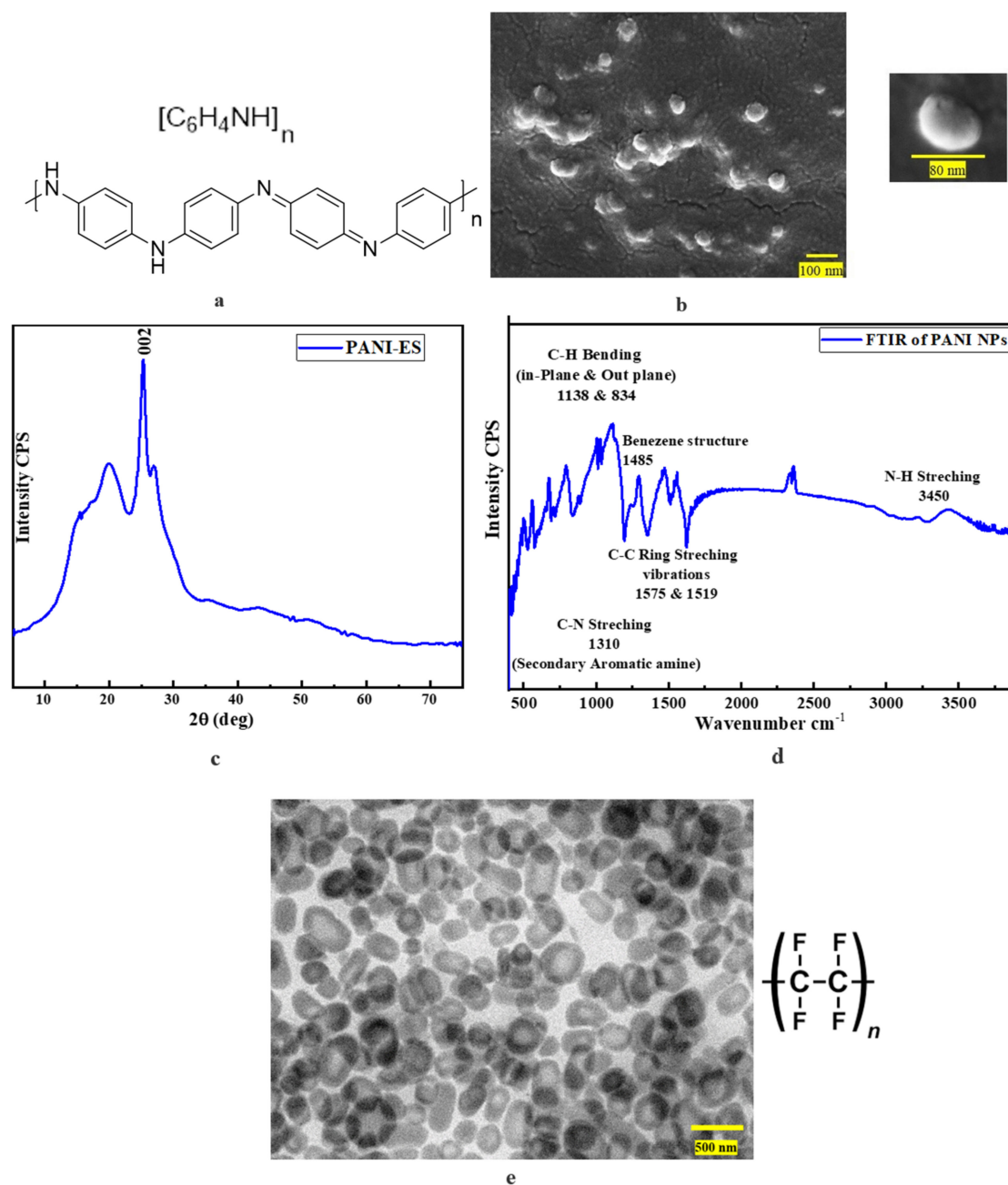


**Figure 1.** PANI particles; (a) Chemical structure; (b) FESEM micrographs; (c) XRD spectra; (d) FTIR spectra (e) PTFE particles micrograph and chemical structure.

## 2. Materials and Methods

### 2.1. PANI Nanoparticles (NPs)

The polyaniline NPs, (PANI-ES) (emeraldine salt) having true density ( $g/cm^3$ ) of  $1.39 g/cm^3$  and a melting point ( $^\circ C$ )  $> 350^\circ C$  were purchased from Aadarsh Innovations, Pune, India, coded as (P). The morphological features of the PANI NPs were probed using a field emission scanning electron microscope (FESEM). The NPs were dispersed in a suitable medium (acetone) and ultrasonicated for deagglomeration. The small drop of the suspension was then placed over carbon tape, followed by drying and acquiring on FESEM micrographs. The micrographs revealed the morphology and size of NPs, as shown in Figure 1b. The NPs appear to have an ovular shape with a size in the range of 70–80 nm.

Furthermore, the X-ray diffraction pattern of polyaniline NPs was acquired using Analytical ( $Cu K\alpha$ ,  $\lambda = 1.5406 \text{ \AA}$ ) at a scanning rate of  $2^\circ \text{ min}^{-1}$  over a  $2\theta$  range of

5° to 75. The diffraction pattern in Figure 1c shows major characteristic peaks at 25.2 (2 $\theta$ ) corresponding to lattice indices (002) reflecting crystallographic planes of PANI. The broader peak centered around 20.2 (2 $\theta$ ) revealed the semi-crystalline nature (amorphous structure~ 020 lattice indices) of PANI NPs. The interlayer spacing ( $d \sim 0.35$  nm) and crystalline size ( $D \sim 0.188$  nm) of PANI NPs was measured from Bragg's law  $n\lambda = 2d \sin\theta$ , where  $\lambda$  is the X-ray wavelength ( $\lambda = 1.5406$  Å),  $d$  is the spacing of the crystal layers,  $\theta$  is the incident angle (the angle between the incident ray and the scattering plane), and  $n$  is an integer [38]. Figure 1c reveals the FTIR spectrum acquired using (Thermo NICOLET-IS 50) FTIR spectrometer over scanning range from 400–4000  $\text{cm}^{-1}$ . The peak at 1308–1340  $\text{cm}^{-1}$  is attributed to C-N stretching of the secondary aromatic amine. The peaks at 1502 and 1592  $\text{cm}^{-1}$  were attributed to C=C stretching of the benzenoid and quinoid moieties, respectively. The peak at 2877  $\text{cm}^{-1}$  is due to C-H asymmetrical stretching. The broad peak in-between 3006–3417  $\text{cm}^{-1}$  corresponds to N-H stretching vibrations of the secondary amine group and N-H stretching in the PANI [39].

### 2.2. PTFE NPs

Polytetrafluoroethylene (PTFE), a synthetic fluoropolymer, is widely used as a solid lubricant owing to its distinctive antifriction properties. PTFE particles with a primary size of  $\sim 200$  nm in the form of suspension were procured from Shamrock, China. These particles are already well characterized in our previous work [12]. A micrograph is shown in Figure 1e that reveals its shape as closer to an oval with a variable size of (180–280 nm) with an average size of around 230 nm.

### 2.3. Base Oils Selected for Preparing Nano-Oils

A Group III mineral oil, as per American petroleum institute (API) classification containing  $S < 10$  ppm, with a density ( $\sim 0.83$  g/cc) viscosity index greater than 125, and kinematic viscosity of base oil at 40 °C (35.4 cSt) and 100 °C (6.3 cSt), was selected as a base stock for preparing Nano-oils. A commercial ashless dispersant comprised (1000 MW mono and bis succinimide) polyisobutylene succinimide (PIBSI) and polyisobutylene succinic anhydride (PIBSA) was employed in base oil served to stabilize the dispersion of NPs. A commercial engine oil (5W30) having density ( $\sim 0.855$  g/cc) and kinematic viscosity (65 cSt) at 40 °C and 11 cSt at 100 °C was also used as a base oil to formulate nano-oils.

### 2.4. Nano-Oils Formulation

The polyaniline NPs were dispersed primarily in API Group III mineral oil with 1 wt.% of commercial dispersant containing a combination of polyisobutylene (PIBSI), and polyisobutylene amide (PIBSA) was used in formulations for enhancing dispersion stability. The compositions of the nano-oils series formulated with mineral oil with varying % of NPs (1–4%), along with codes, are shown in Table 1. A commercial 5W-30 oil was used for the engine oil series, and the concentration of NPs varied from 1–4%, and four nano-oils were formulated similar to the mineral oil series. An additional two hybrid oils comprised of NPs of PTFE and PANI in the ratio of 3:1 and 2:1 were also developed in order to observe any synergism.

The nano oils were formulated using a simplified methodology as shown through the schematic in Figure 2, along with the photographs of PANI-based mineral nano oils.

The process involved weighing the desired amount of NPs and adding to base/engine oil. It is noted that 1 wt.% of dispersant was added in mineral oil and hybrid oil, whereas it was not added to the engine oil series to avoid incompatibility with the existing dispersant. These were ultrasonicated by a combination of magnetic stirring and probe sonication for 5 min until the desired wt.% was dispersed in the oils. Finally, ultrasonication for 30 min was carried out using a probe sonicator (UP 800, E-Chrom Tech. Taiwan) to homogenize the dispersion and make stable nano oils. The nano-oils prepared in mineral oil were stable for more than one week. While formulating nano-oils using a probe sonicator, precautions

were taken not to exceed temperatures beyond 25 °C by using an ice trap around the beaker containing the nano oil.

**Table 1.** Nano-oils using two base oils.

Series	Oil Codes	Codes-Nano-Oils				
1	Mineral oil (Grp III) Series + 1% (PIBSI + PIBSA)	O <sup>#</sup>	P <sub>1</sub>	P <sub>2</sub>	P <sub>3</sub>	P <sub>4</sub>
2	Engine oil (SAE 5W30) Series	E <sup>#</sup>	EP <sub>1</sub>	EP <sub>2</sub>	EP <sub>3</sub>	EP <sub>4</sub>
3	Hybrid oil (H) Series- + 1% (PIBSI + PIBSA)	H	-	-	T <sub>2</sub> P <sub>1</sub>	T <sub>3</sub> P <sub>1</sub>

O ~ Mineral oil, O<sup>#</sup> ~ Mineral oil + dispersant 1 wt.% (PIBSI +PIBSA), E<sup>#</sup>~ Engine oil; P for polyaniline and T~ Polytetrafluoroethylene/PTFE NPs; Subscripts '1', '2', '3', '4', denote the wt.% of NPs.

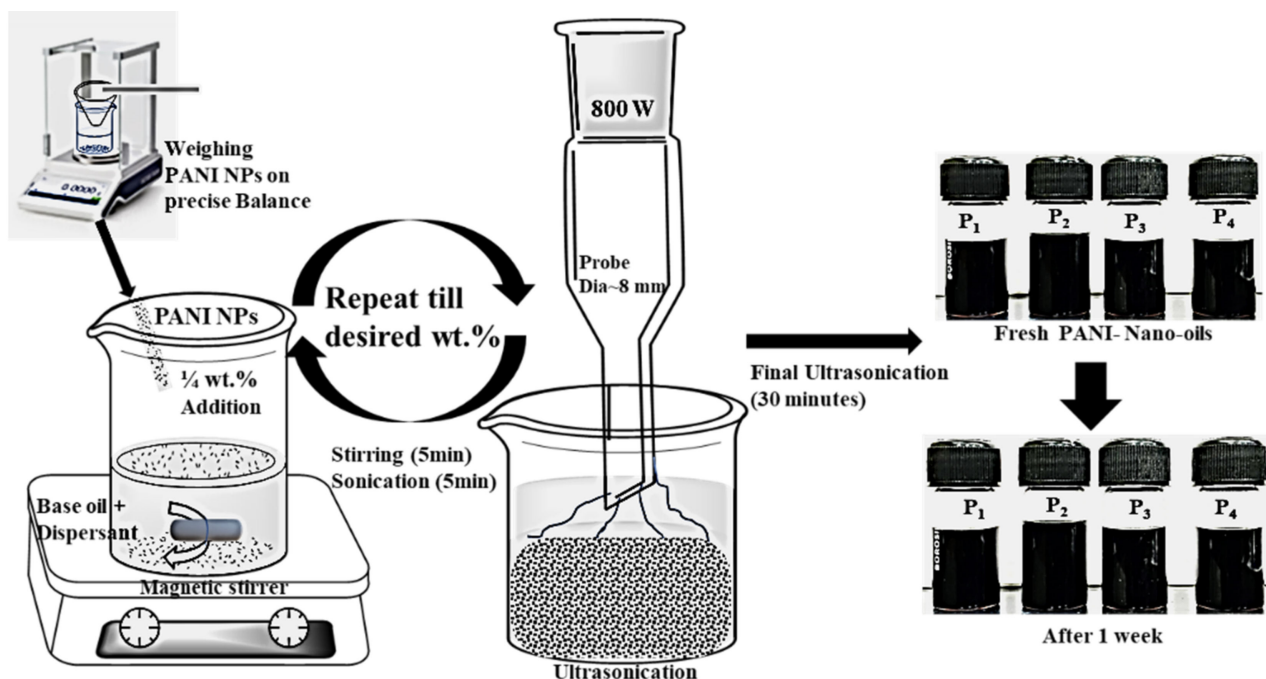


**Figure 2.** The formulation process of PANI-nano oils using mineral oils.

### 2.5. Thermal Properties

One of the essential applications of lubricants is the high capability of heat transmission and it is important to keep the oil cool so that oxidation will be minimal. In internal combustion engines, for instance, the primary function of lubricants is to decrease friction and wear, but they also play a crucial role in heat transmission. The thermal conductivity (TC) of base oil and P<sub>3</sub> oil was measured using a DTC 300 Thermal Conductivity Analyzer (TA instruments).

The TC of base oil and a nano oil (P<sub>3</sub>) was measured in the temperature range (30–105 °C), and the data in the form of the graph are shown in Figure 3. The addition of PANI NPs significantly enhanced the TC of oils, especially at the highest selected temperature (105 °C); the difference in TC was 30%. This can primarily be attributed to the exceptionally high TC of PANI NPs (~3000 W/m·°C) [40].

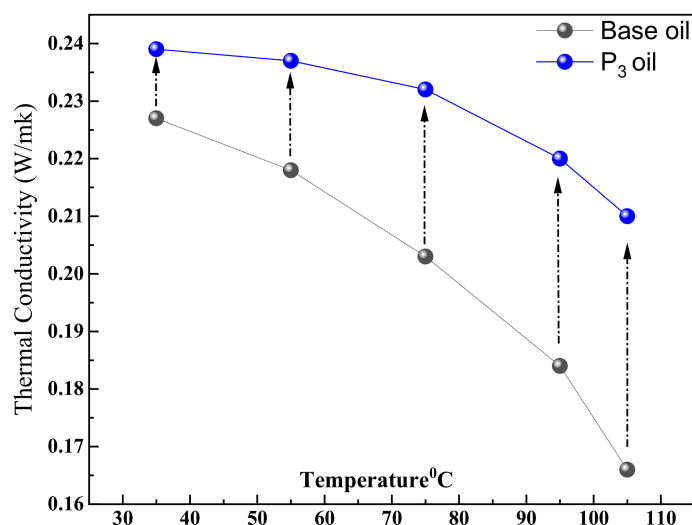


**Figure 3.** Thermal conductivity (TC) of base oil and P<sub>3</sub> oil as a function of temperature.

### 2.6. Tribological Performance Evaluation of Developed Oil Samples

On a pneumatic fourball tester supplied by Ducom Bangalore, the tribological performance (antiwear and extreme pressure) of oils was evaluated per ASTM D-4172 [41] and IP-239 [42] test standards. During experiments, in every single test run, four new identical spherical steel balls (D~12.7 mm, Ra 35 nm, and HRC (65–70) made of AISI-52100 chromium-enriched steel) were employed. Before the test runs, these steel balls were ultrasonically cleaned in hexane to remove any surface impurities. In this setup, the three balls were dipped in lubricant to be tested and held tightly in place inside the ball-pot. While the fourth ball is held firmly inside spindle that rotates at the desired speed over the dipped balls under load, as shown in Figure 4, depicts the fourball tester's schematic.

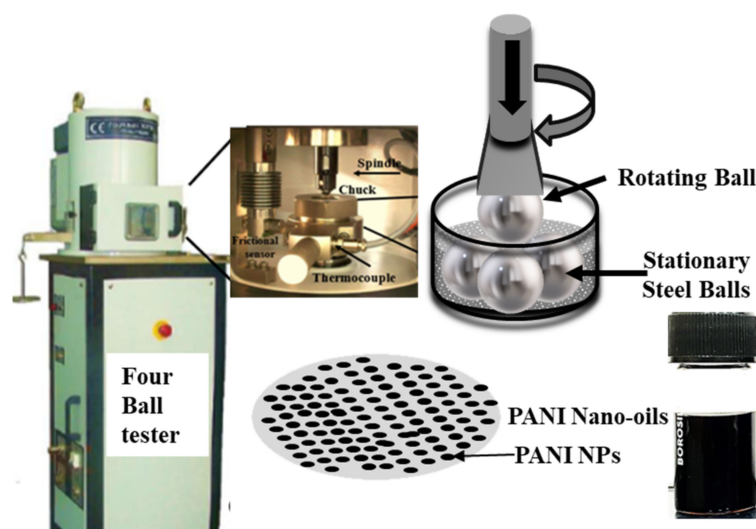


**Figure 4.** Fourball tester machine and its schematics.

In an AW test on the formulated oils, 40 kg load was applied, and the top ball attached to the spindle was rotated at 1200 rpm for 1 h. After the test, balls were cleaned, and wear scars (WSD) were measured. Three test runs were conducted, and the average of the three WSDs formed served as the final WSD value for the examined oil. EP property measures the load-bearing capacity of lubricants under extreme pressure and at 1450 rpm for a specified period (10, 60 s). For the evaluation of EP property, the IP-239 EP standard was employed. The test comprises a series of 60-s experiment runs conducted at progressively increasing loads until the breakdown of the lubricant film causes the seizure of metallic

asperities or the welding of balls. The weld load refers to the final load stage before failure, accompanied by an immediate increase in friction torque and noise level. Three iterative test runs at pre-weld and weld load was used to ascertain the extreme pressure properties of formulated NLs.

### 3. Results and Discussion

#### 3.1. Influence on EP Property of Oils

The load-bearing capacity of oils is a crucial indicator of lubricant performance under extreme temperatures and load conditions. The EP performance of oils measured from the IP-239 test is illustrated in the bar graph in Figure 5. The base oil contained 1 wt.% of dispersant (coded as O<sup>#</sup> had the same weld load of 126 kg as a virgin base oil (O).

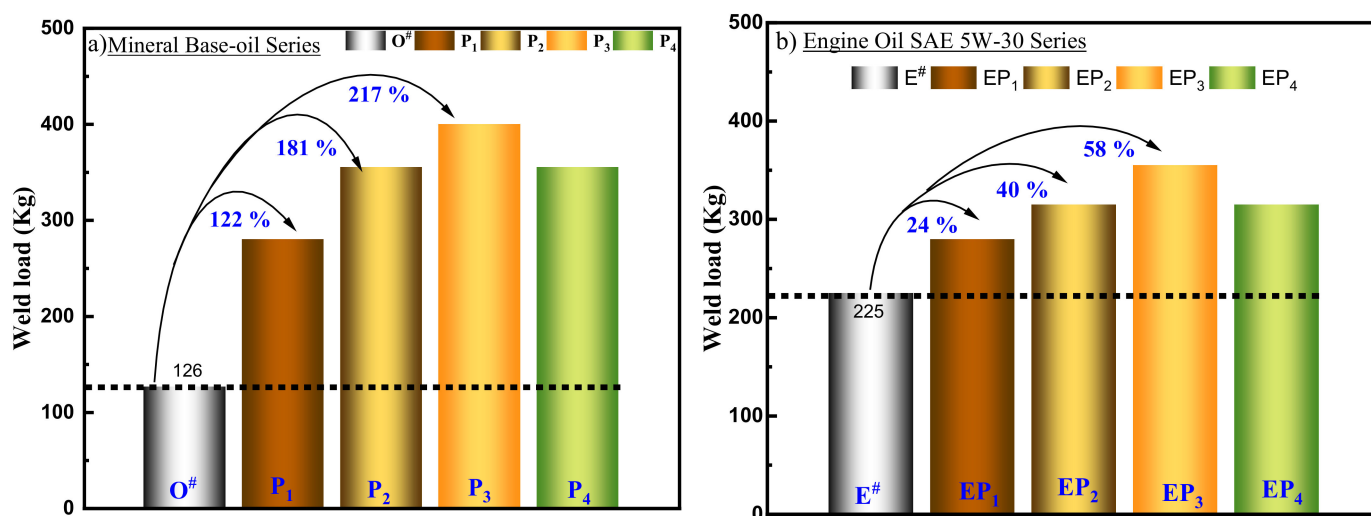


**Figure 5.** EP properties (weld-load) of nano-oils Series; (a) Series 1- Mineral oil based; (b) Series 2- Engine oil-based.

The inclusion of PANI NPs in both mineral oil and engine oil significantly improved the load-carrying ability of oils. The trends in percentage improvement reveals gradual increment in the EP performance of PANI nano oils till 3 wt.%. Similar trends of decrease in EP performance after optimal concentration are reported for different NPs [14,43].

- For Mineral Oils; P<sub>3</sub> (217%) > P<sub>2</sub> (181%) > P<sub>4</sub> (11%) ~ P<sub>1</sub> (122%) > O<sup>#</sup>
- For Engine Oils; EP<sub>3</sub> (58%) > EP<sub>2</sub> (40%) > EP<sub>4</sub> (40%) ~ EP<sub>1</sub> (24%) > E<sup>#</sup>

Nearly 220% and 60% increments were observed with the mere addition of PANI NPs in mineral oil and engine oil. The 3% was the optimized amount since the highest improvement was observed in both series. This can be attributed to enhanced heat dissipation due to the higher TC of nano-oils and triggered release of PANI NPs in the rubbed area, valleys, and asperities to form a tribofilm, as discussed in subsequent sections. Similar trends of decrease in EP performance after optimal concentration are reported for different NPs [14,43].

#### Tribo-Films Characterization on Worn Surface Pre-Weld Balls of PANI-Nano-Oils

Generally, most of the conventional EP additives work by forming a sacrificial chemical adsorbed film over the contacting surface but only after attaining specific temperature and pressure conditions requisite for the additive to get activated. In contrast, the NPs in oil, as EPA work by forming a combination of chemisorbed and physisorbed film over the surface when smeared during rubbing [23,44,45]. In general, at an optimized concentration of NPs, the lubrication behaviours of NPs are shown through the schematic in Figure 6.

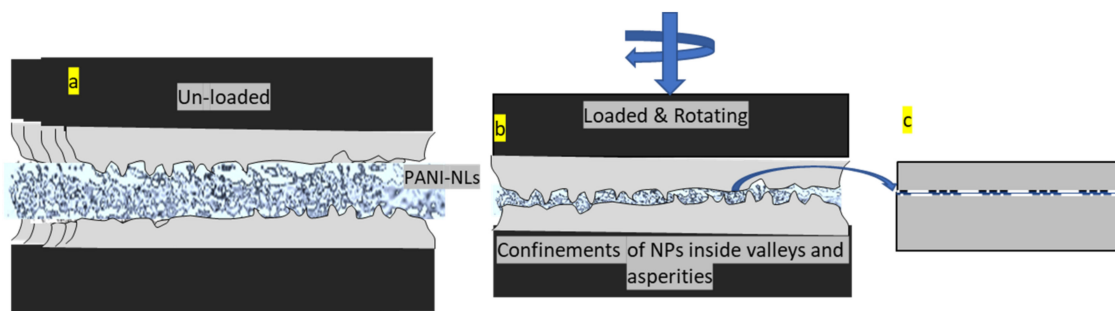


**Figure 6.** Generalized lubrication behavior of NPs during extreme pressure conditions. (a) Unloaded asperities and a thick layer of nano oil; (b) loaded asperities during tribo-test and a thin layer of nano-oil; and (c) physical and chemical interaction of NPs with asperities leading to the formation of the thin coherent film.

The contact strength of formed tribofilm is mainly responsible for EPA performance; how fast this film gets developed over the contacting interphase varies upon the reaction kinematics of NPs to interact with exposed surfaces [45,46]. The SEM micrographs ( $1000\times$ ) of worn surfaces of the balls at pre-weld loads are shown for  $P_2$ ,  $P_3$ , and  $P_4$  nano-oils, along with respective elemental maps of the contributing additives (Carbon) in Figure 7.

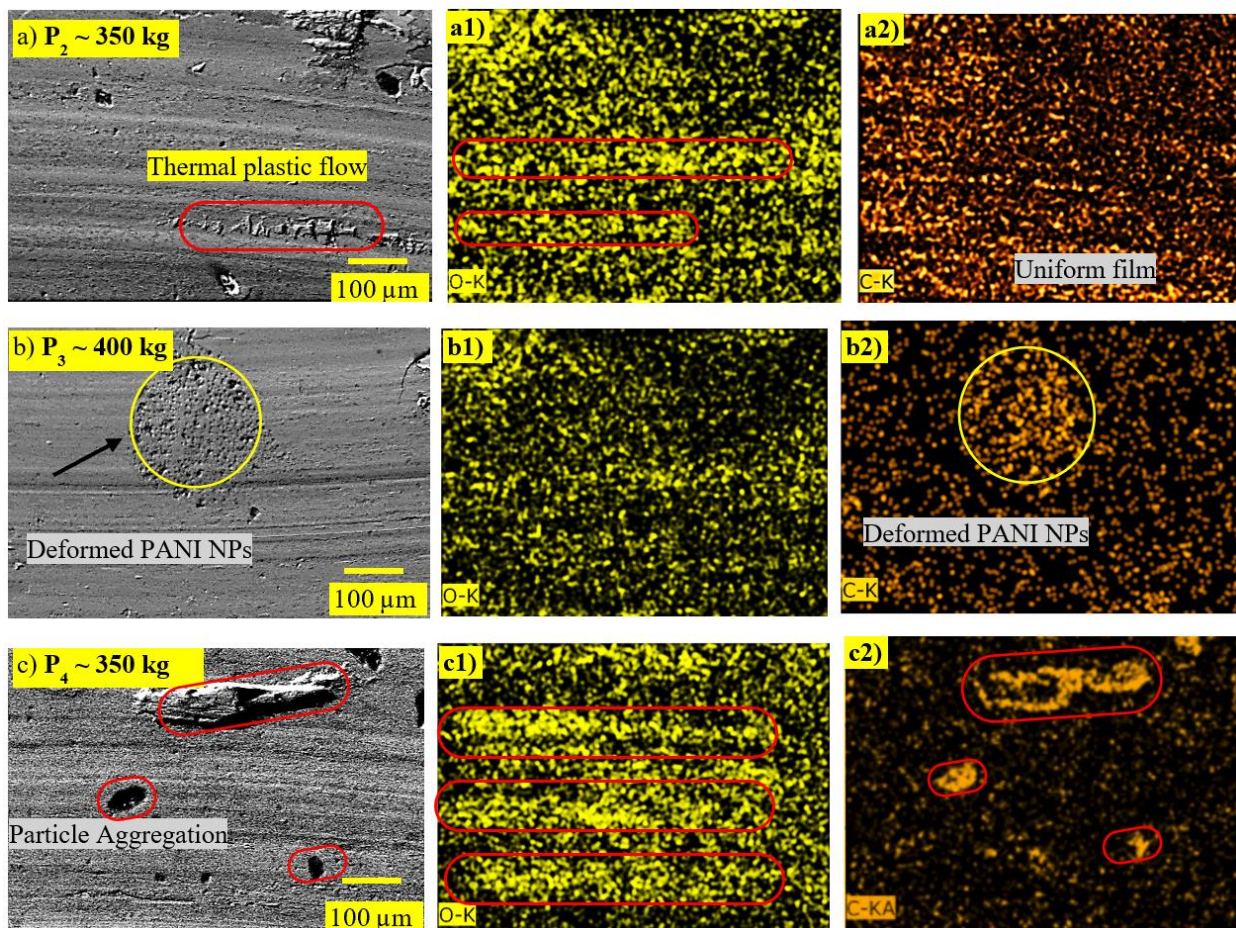


**Figure 7.** SEM micrographs ( $1000\times$ ) of the worn ball samples at pre-weld loads; (a)  $P_2$ ; (b)  $P_3$ ; and (c)  $P_4$ ; along with elemental dot maps of representative elements (O) at (a1–c1) and (C) at (a2–c2).

The worn surfaces of the balls revealed abrasion marks along the sliding direction. The surfaces of the balls lubricated with  $P_2$ ,  $P_4$  showed thermal scratch marks, aggregated particles as highlighted inside the red area in micrographs 7a1 and 7c1 respectively indicat-

ing less coherent films on the surfaces. On the other hand, micrograph 7b1 shows smoother topography without abrasion marks and evidence of a cluster of deformed NPs in the highlighted area inside (yellow circle Figure 7b) supported by higher C dot map density (micrograph 7b2).

It appears that the nitrogen group in PANI led to anchoring chains with a metallic surface and formed protective films over the surface that led to enhancement in the load bearing ability of nano oils. It reported [47,48] that metallic surfaces form Iron oxides ( $\text{FeO}$ ,  $\text{Fe}_2\text{O}_3$ , and  $\text{Fe}_3\text{O}_4$ ) during sliding. The oxygen map reveals the oxidation of metallic asperities in contacts during sliding. The lower dot density indicates a lower extent of oxidation vis-à-vis the lower extent of heat generated and, in short, the superiority of oil. The elemental map of Oxygen in micrograph 7b2 revealed the lowest amount of oxygen coverage, followed by 7a2. The highest oxidation was shown by  $\text{P}_4$  oil, as highlighted red area inside observed on Figure 7c1. This supported the best behavior of  $\text{P}_3$  oil.

### 3.2. Antiwear (AW.) Performance of Nano-Oils

The antiwear (AW) performance of PANI nano-oils formulated with mineral oils is represented in the form of the average wear scar diameter (WSD) of static balls in Figure 8.

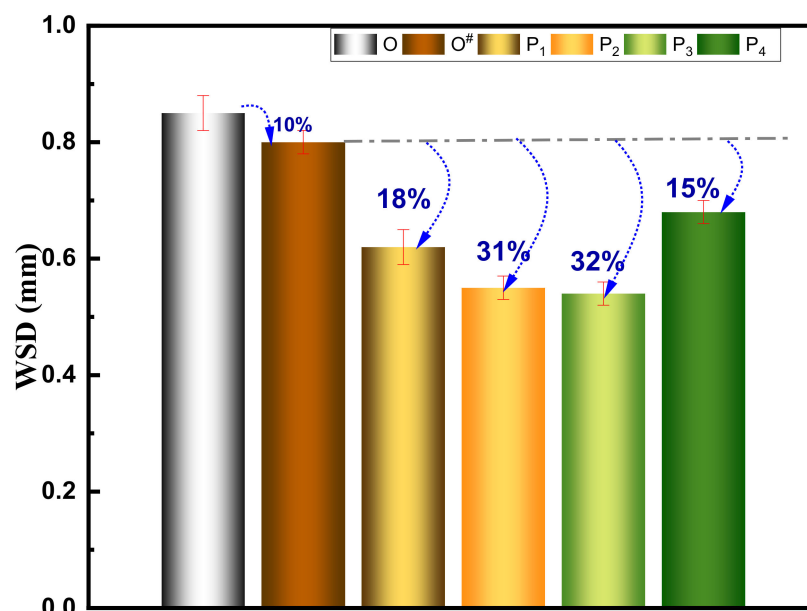
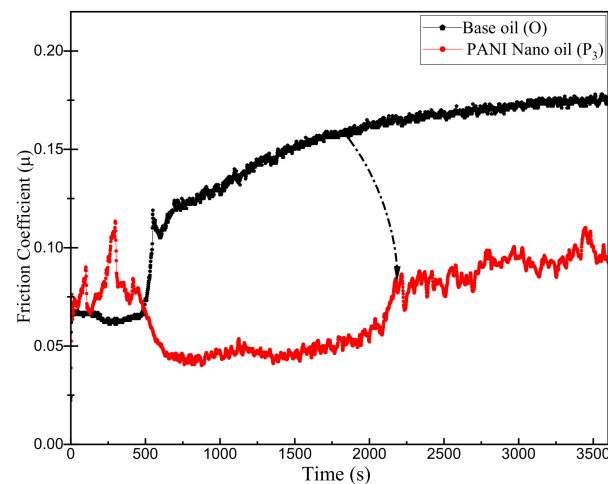


Figure 8. Anti Wear performance of PANI NPs compared to the base oil with dispersant.

The addition of NPs led to a gradual increase in the wear-preventive behavior of mineral oils, thereby proving their potential as replacement AWA additives. The effect of the selected dispersant in lowering the WSD (~6 wt.%) for base oil is reported in our previous work [23,48]. However, some dispersants beyond 1 wt.% tend to hinder the wear-preventive characteristics of base oils [49]. Thus, the optimal amount of dispersant must be employed during formulation. Therefore, performance enhancement reported trends reported in Figure 8 were measured concerning dispersant-added oil  $\text{O}^\#$ . Overall, the performance order for PANI Nano-oils in terms of its AW performance compared to base oil with dispersant was as follows:  $\text{P}_3$  (32%) >  $\text{P}_2$  (31%) >  $\text{P}_1$  (18%) >  $\text{P}_4$  (15%) >  $\text{O}^\#$

NPs up to 2–3 wt.% led to the best results. Overall, the 3 wt.% was found to be the optimal concentration for both AWA and EPA. The comparative friction performance is also shown in Figure 9.



**Figure 9.** Friction performance comparison of PANI ( $P_3$ ) nano-oil.

The friction curve shows fluctuations in  $\mu$  initially during the run-in period and varied from  $\sim (0.07$  to  $0.10)$  during the first 500 s, whereas it was stable for base oil with  $\mu \sim 0.7$ . This can be attributed to the stable flow of base oil initially, whereas NPs, which do not have lamellar structure hinder the sliding during run-in for 500 s. However, after 500 s, the base oil  $\mu$  curve rose steadily ( $\sim 0.11$ ), which can be ascribed to the break of the lubricant film due to the rise in contact temperature. This might have led to severe abrasion, and accelerated wear of the ball surface led to the continuous rise in  $\mu \sim 0.14$ . However, the opposite trend was observed in the case of PANI NLs; the  $\mu$  decreased after 500 s stabilizing to  $\sim 0.05$  till 2100 s with negligible fluctuations. This can be ascribed to the gradual deformation of PANI NPs that led to carbonaceous film responsible for lower friction. However, gradual sliding after 2200 s led to gradual formation and removal of films, corresponding to a rise in  $\mu \sim 0.07$  and fluctuations for PANI NLs. Overall, the friction performance of PANI nano oils corroborates its enhanced wear preventive behavior. The worn surface analysis over the formed film is presented in the subsequent sections to confirm the lubrication mechanism.

#### Antiwear Tribo-Film Analysis on Balls Lubricated with Combo Oils

To quantify the composition of the transfer film, a Renishaw (INVIA), a Raman spectrometer with a 532 nm laser, was used to examine the worn surfaces lubricated with PANI nano oil ( $P_3$ ) and raw PANI NPs. Around 30 Raman spectra were accumulated for an exposure time of 10 s at 10 mW laser power, and the obtained spectra are shown in Figure 10.

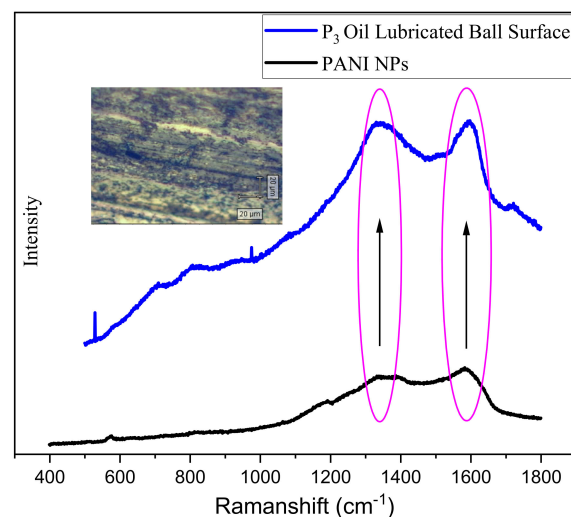


**Figure 10.** Tribo film formed by PANI NPs over the worn surface.

The Raman spectra obtained for PANI NPs reveal peaks corresponding to C-N, C-H bending stretching at 1331, and C-C stretching of the benzene ring at 1590  $\text{cm}^{-1}$ . However, the higher intensity of the peaks found at the worn surface of the ball lubricated with PANI Nano oils suggested deformation of PANI NPs to carbonaceous films showing more like typical (disorder) D and (Graphitic) G bands peaks [50]. Similar D and G bands peaks have been reported earlier that behave like an amorphous carbon layer [17,21,27,51,52] and provide better wear preventive characteristics to oils.

### 3.3. Hybrid Oil EP Performance

The EP performance of formulated hybrid oils is shown in Figure 11. The value of weld load for  $T_3$  (3% NPs of PTFE) is added from the literature [20]. Comparative results indicate that the addition of PTFE NPs along with PANI NPs in 2:1, 3:1 ratio resulted in tribo-synergism in EP performance, which increased the weld load to ~ 455% and 535% compared to the base oil. The lubrication mechanism of PTFE to work as excellent EPA (chain scission-C-C- and /-C-F- bonds at higher loads) is well established, as reported in previous work [20] for oils and greases [16,53]. It was interesting to compare the performance of excellent additives used in the literature as EPA, as shown in Figure 11b. Clearly, hybrid oils of PANI and PTFE in unique combinations outperformed other NPs as EPA.

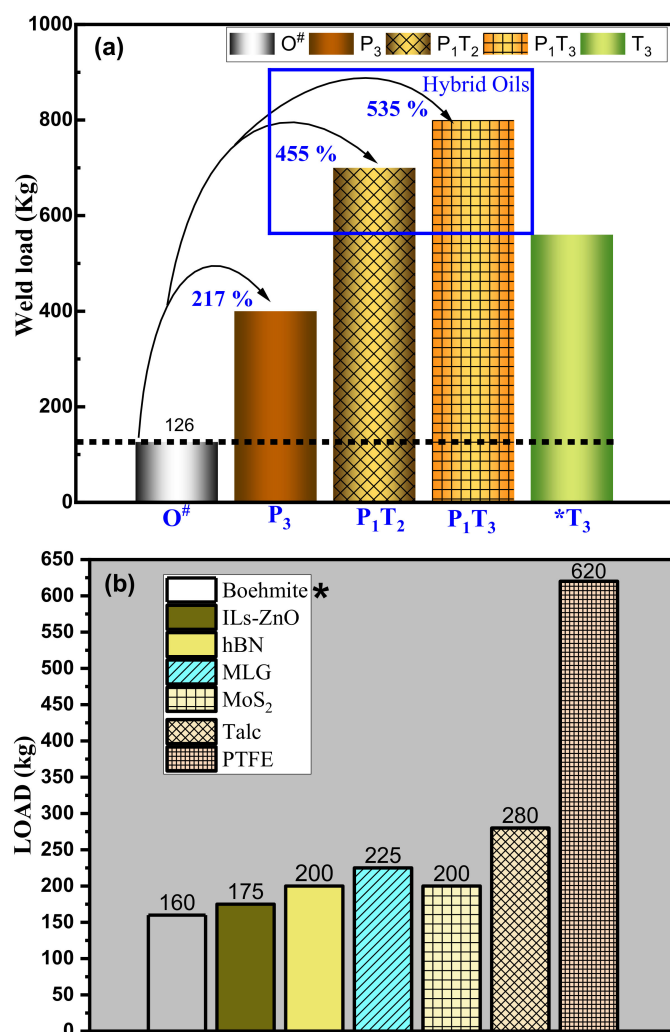


**Figure 11.** (a) EP Performance of Hybrid oils \* ( $T_3 \sim 560$  kg weld load [20]) and (b) extracts from the literature on the weld load of different nano oils using mineral oils (Group I, II, III and IV) as base oils. \* (Boehmite [54], ILs ZnO [15], hBN [49], MLG/Graphite [27], MoS<sub>2</sub> [55], Talc [23], PTFE [20]).

#### 4. Conclusions

This research demonstrated that the formulations of novel nano oils using PANI nanoparticles are capable of improving the thermal and tribological performance of oils to a large extent. The mineral and engine-based series revealed the optimum concentration in the selected range viz. 1–4% of PANI NPs needed for the highest tribo-performance. EPA PANI-based NLs demonstrated significant enhancement: ~217% and 58% for mineral and engine oil base series, respectively. When employed as AWA, the PANI NPs also showed their capability in enhancing the (~32%) wear preventive characteristics of mineral oils. The tribo-film formed due to sheared deformation that led to the formation of the amorphous carbonaceous layer, being accountable for a reduction in friction and wear. The addition of PANI led to an increase in the thermal conductivity of mineral oils, which reflects enhanced heat dissipation ability. Moreover, polymeric PANI nanoparticles can easily be synthesized, rendering them an affordable choice. The work also reveals a unique combination of PTFE with PANI NPs in a ratio of 3:1, yielding the highest EP performance enhancement ~535% ever reported in the literature.

#### 5. Patents

The above work is a part of Indian Patent Application No. 202211033059 (9.06.2022) entitled “AN ADDITIVE TO IMPROVE THE TRIBO-PERFORMANCE OF ENGINE OILS, GEAR OILS AND GREASES” in the name of INDIAN INSTITUTE OF TECHNOLOGY DELHI 202211033059 dated 9 June 2022 submitted by the authors

**Author Contributions:** Conceptualization, V.S. and J.B.; methodology, V.S. and J.B.; formal analysis, V.S.; investigation, V.S.; resources, J.B.; data curation, V.S.; supervision, J.B. All authors have read and agreed to the published version of the manuscript.

**Funding:** This research received no external funding.

**Data Availability Statement:** Not applicable.

**Conflicts of Interest:** The authors declare that they have no conflicts of interest.

#### References

1. Jha, S.; Nanda, S.; Acharya, B.; Dalai, A.K. A Review of Thermochemical Conversion of Waste Biomass to Biofuels. *Energies* **2022**, *15*, 6352. [[CrossRef](#)]
2. Zhang, M.; Wang, X.; Fu, X.; Xia, Y. Performance and Anti-Wear Mechanism of CaCO<sub>3</sub> Nanoparticles as a Green Additive in Poly-Alpha-Olefin. *Tribol. Int.* **2009**, *42*, 1029–1039. [[CrossRef](#)]
3. Arora, A.; Jha, S.; Saini, V. Aspects of Green-Sustainable Tribology and Its Impacts on Future Product Development: A Review. *Ecol. Environ. Conserv.* **2019**, *25*, S146–S157.
4. Morshed, A.; Wu, H.; Jiang, Z. A Comprehensive Review of Water-Based Nanolubricants. *Lubricants* **2021**, *9*, 89. [[CrossRef](#)]
5. Akl, S.; Elsoudy, S.; Abdel-Rehim, A.A.; Salem, S.; Ellis, M. Recent Advances in Preparation and Testing Methods of Engine-Based Nanolubricants: A State-of-the-Art Review. *Lubricants* **2021**, *9*, 85. [[CrossRef](#)]
6. Okokpuije, I.P.; Tartibu, L.K.; Sinebe, J.E.; Adeoye, A.O.M.; Akinlabi, E.T. Comparative Study of Rheological Effects of Vegetable Oil-Lubricant, TiO<sub>2</sub>, MWCNTs Nano-Lubricants, and Machining Parameters' Influence on Cutting Force for Sustainable Metal Cutting Process. *Lubricants* **2022**, *10*, 54. [[CrossRef](#)]
7. Martin, J.M.; Ohmae, N. *Nanolubricants*; John Wiley & Sons: London, UK, 2008.
8. Gulzar, M.; Masjuki, H.H.; Kalam, M.A.; Varman, M.; Zulkifli, N.W.M.; Mufti, R.A.; Zahid, R. Tribological Performance of Nanoparticles as Lubricating Oil Additives. *J. Nanoparticle Res.* **2016**, *18*, 1–25. [[CrossRef](#)]
9. Dai, W.; Kheireddin, B.; Gao, H.; Liang, H. Roles of Nanoparticles in Oil Lubrication. *Tribol. Int.* **2016**, *102*, 88–98. [[CrossRef](#)]
10. Fan, X.; Li, W.; Fu, H.; Zhu, M.; Wang, L.; Cai, Z.; Liu, J.; Li, H. Probing the Function of Solid Nanoparticle Structure under Boundary Lubrication. *ACS Sustain. Chem. Eng.* **2017**, *5*, 4223–4233. [[CrossRef](#)]
11. Rasheed, A.K.K.; Khalid, M.; Rashmi, W.; Gupta, T.C.S.M.; Chan, A. Graphene Based Nanofluids and Nanolubricants—Review of Recent Developments. *Renew. Sustain. Energy Rev.* **2016**, *63*, 346–362. [[CrossRef](#)]
12. Saini, V.; Bijwe, J.; Seth, S.; Ramakumar, S.S.V. Role of Base Oils in Developing Extreme Pressure Lubricants by Exploring Nano-PTFE Particles. *Tribol. Int.* **2020**, *143*, 106071. [[CrossRef](#)]
13. Gupta, R.N.; Harsha, A.P.; Singh, S. Tribological Study on Rapeseed Oil with Nano-Additives in Close Contact Sliding Situation. *Appl. Nanosci.* **2018**, *8*, 567–580. [[CrossRef](#)]

14. Solanki, R.; Saini, V.; Bijwe, J. Exploration of PTFE Sub-Micron Particles for Enhancing the Performance of Commercial Oils. *Surf. Topogr. Metrol. Prop.* **2021**, *9*, 025005. [[CrossRef](#)]
15. Maurya, U.; Vasu, V.; Kashinath, D. Ionic Liquid-Nanoparticle-Based Hybrid-Nanolubricant Additives for Potential Enhancement of Tribological Properties of Lubricants and Their Comparative Study with ZDDP. *Tribol. Lett.* **2022**, *70*, 11. [[CrossRef](#)]
16. Gupta, T.; Kumar, A.; Prasad, B. Sustainable Lubrication: Low Molecular Weight PTFE Micro-Particles as Extreme Pressure Additives for Heavy Duty Grease Applications. *Ind. Lubr. Tribol.* **2021**, *73*, 1209–1218. [[CrossRef](#)]
17. Kumar, N.; Saini, V.; Bijwe, J. Tribological Investigations of Nano and Micro-Sized Graphite Particles as an Additive in Lithium-Based Grease. *Tribol. Lett.* **2020**, *68*, 124. [[CrossRef](#)]
18. Rawat, S.S.; Harsha, A.P.; Deepak, A.P. Tribological Performance of Paraffin Grease with Silica Nanoparticles as an Additive. *Appl. Nanosci.* **2019**, *9*, 305–315. [[CrossRef](#)]
19. Lee, K.; Hwang, Y.; Cheong, S.; Choi, Y.; Kwon, L.; Lee, J.; Kim, S.H. Understanding the Role of Nanoparticles in Nano-Oil Lubrication. *Tribol. Lett.* **2009**, *35*, 127–131. [[CrossRef](#)]
20. Saini, V.; Bijwe, J.; Seth, S.; Ramakumar, S.S.V. Interfacial Interaction of PTFE Sub-Micron Particles in Oil with Steel Surfaces as Excellent Extreme-Pressure Additive. *J. Mol. Liq.* **2021**, *325*, 115238. [[CrossRef](#)]
21. Ye, Q.; Liu, S.; Zhang, J.; Xu, F.; Zhou, F.; Liu, W. Superior Lubricity and Antiwear Performances Enabled by Porous Carbon Nanospheres with Different Shell Microstructures. *ACS Sustain. Chem. Eng.* **2019**, *7*, 12527. [[CrossRef](#)]
22. Sgroi, M.F.; Asti, M.; Gili, F.; Deorsola, F.A.; Bensaid, S.; Fino, D.; Kraft, G.; Garcia, I.; Dassenoy, F. Engine Bench and Road Testing of an Engine Oil Containing MoS<sub>2</sub> Particles as Nano-Additive for Friction Reduction. *Tribol. Int.* **2017**, *105*, 317–325. [[CrossRef](#)]
23. Saini, V.; Bijwe, J.; Seth, S.; Ramakumar, S.S.V. Potential Exploration of Nano-Talc Particles for Enhancing the Anti-Wear and Extreme Pressure Performance of Oil. *Tribol. Int.* **2020**, *151*, 106452. [[CrossRef](#)]
24. Kumar, N.; Saini, V.; Bijwe, J. Exploration of Talc Nanoparticles to Enhance the Performance of Lithium Grease. *Tribol. Int.* **2021**, *162*, 107107. [[CrossRef](#)]
25. Rudenko, P.; Bandyopadhyay, A. Talc as Friction Reducing Additive to Lubricating Oil. *Appl. Surf. Sci.* **2013**, *276*, 383–389. [[CrossRef](#)]
26. Eswaraiiah, V.; Sankaranarayanan, V.; Ramaprabhu, S. Graphene-Based Engine Oil Nanofluids for Tribological Applications. *ACS Appl. Mater. Interfaces* **2011**, *3*, 4221–4227. [[CrossRef](#)]
27. Saini, V.; Seth, S.; Ramakumar, S.S.V.; Bijwe, J. Carbon Nanoparticles of Varying Shapes as Additives in Mineral Oil Assessment of Comparative Performance Potential. *ACS Appl. Mater. Interfaces* **2021**, *13*, 38844–38856. [[CrossRef](#)]
28. Berman, D.; Erdemir, A.; Sumant, A.V. Graphene: A New Emerging Lubricant. *Mater. Today* **2014**, *17*, 31. [[CrossRef](#)]
29. Asadauskas, S.J.; Kreivaitis, R.; Bikulčius, G.; Grigučevičienė, A.; Padgurskas, J. Tribological Effects of Cu, Fe and Zn Nanoparticles, Suspended in Mineral and Bio-Based Oils. *Lubr. Sci.* **2016**, *28*, 157–176. [[CrossRef](#)]
30. Gupta, M.K.; Bijwe, J.; Padhan, M. Role of Size of Hexagonal Boron Nitride Particles on Tribo-Performance of Nano and Micro Oils. *Lubr. Sci.* **2018**, *30*, 441–456. [[CrossRef](#)]
31. Osama, M.; Singh, A.; Walvekar, R.; Khalid, M.; Gupta, T.C.S.M.; Yin, W.W. Recent Developments and Performance Review of Metal Working Fluids. *Tribol. Int.* **2017**, *114*, 389–401. [[CrossRef](#)]
32. Ilyas, S.U.; Ridha, S.; Sardar, S.; Estellé, P.; Kumar, A.; Pendyala, R. Rheological Behavior of Stabilized Diamond-Graphene Nanoplatelets Hybrid Nanosuspensions in Mineral Oil. *J. Mol. Liq.* **2021**, *328*, 115509. [[CrossRef](#)]
33. Khare, V.; Pham, M.Q.; Kumari, N.; Yoon, H.S.; Kim, C.S.; Park, J. II; Ahn, S.H. Graphene-Ionic Liquid Based Hybrid Nanomaterials as Novel Lubricant for Low Friction and Wear. *ACS Appl. Mater. Interfaces* **2013**, *5*, 4063–4075. [[CrossRef](#)]
34. Nasser, K.I.; Liñeira del Río, J.M.; Mariño, F.; López, E.R.; Fernández, J. Double Hybrid Lubricant Additives Consisting of a Phosphonium Ionic Liquid and Graphene Nanoplatelets/Hexagonal Boron Nitride Nanoparticles. *Tribol. Int.* **2021**, *163*, 107189. [[CrossRef](#)]
35. Maurya, U.; Vasu, V. Synergistic Effect Between Phosphonium-Based Ionic Liquid and Three Oxide Nanoparticles as Hybrid Lubricant Additives. *J. Tribol.* **2020**, *142*, 052101. [[CrossRef](#)]
36. Kumar, N.; Saini, V.; Bijwe, J. Synergism or Antagonism in Tribo-Performance of Nano-Greases Using Combinations of Nanoparticles of Graphite and PTFE. *Appl. Nanosci.* **2021**, *11*, 2525–2536. [[CrossRef](#)]
37. Bijwe, J.; Chauhan, V.; Darpe, A. Copper-Free Eco-Friendly Friction Materials/Brake-Pads/Shoes. Indian Patent FT-IDF-12-2020-169, 2021. *Submitted Indian Patent*.
38. Bragg, W.H.; Bragg, W.L. *X-rays and Crystal Structure*; G. Bell and Sons, Limited: London, UK, 1915.
39. Lin-Vien, D.; Colthup, N.B.; Fateley, W.G.; Grasselli, J.G. *The Handbook of Infrared and Raman Characteristic Frequencies of Organic Molecules*; Elsevier: Amsterdam, The Netherlands, 1991; ISBN 0080571166.
40. Ahmadi, Z.; Chauhan, N.P.S.; Zarrintaj, P.; Khiabani, A.B.; Saeb, M.R.; Mozafari, M. Experimental Procedures for Assessing Electrical and Thermal Conductivity of Polyaniline. In *Fundamentals and Emerging Applications of Polyaniline*; Elsevier: Amsterdam, The Netherlands, 2019; pp. 227–258. [[CrossRef](#)]
41. ASTM D4172-21; Standard Test Method for Wear Preventive Characteristics of Lubricating Fluid (Four-Ball Method). ASTM International: West Conshohocken, PA, USA, 2021.
42. IP 239. *Determination of Extreme Pressure and Antiwear Properties of Lubricating Fluids and Greases-Four Ball Method (European Conditions)*; Energy Institute: London, UK, 2014.

43. Mungse, H.P.; Gupta, K.; Singh, R.; Sharma, O.P.; Sugimura, H.; Khatri, O.P. Alkylated Graphene Oxide and Reduced Graphene Oxide: Grafting Density, Dispersion Stability to Enhancement of Lubrication Properties. *J. Colloid Interface Sci.* **2019**, *541*, 150–162. [[CrossRef](#)]
44. Li, H.; Zhang, Y.; Li, C.; Zhou, Z.; Nie, X.; Chen, Y.; Sharma, S. Extreme pressure and antiwear additives for lubricant: Academic insights and perspectives. *Int. J. Adv. Manuf. Technol.* **2022**, *120*, 1–27. [[CrossRef](#)]
45. Mello, V.S.; Trajano, M.F.; Guedes, A.E.; Alves, S.M. Comparison Between the Action of Nano-Oxides and Conventional EP Additives in Boundary Lubrication. *Lubricants* **2020**, *8*, 54. [[CrossRef](#)]
46. Lin, Y.-C.; Cho, Y.-H.; Chiu, C.-T. Tribological Performance of EP Additives in Different Base Oils. *Tribol. Trans.* **2012**, *55*, 175–184. [[CrossRef](#)]
47. Quinn, T.F.J.; Sullivan, J.L.; Rowson, D.M. Origins and Development of Oxidational Wear at Low Ambient Temperatures. *Wear* **1984**, *94*, 175–191. [[CrossRef](#)]
48. Saini, V.; Bijwe, J.; Seth, S.; Ramakumar, S.S.V. Unexplored Solid Lubricity of Titanium Nanoparticles in Oil to Modify the Metallic Interfaces. *Appl. Surf. Sci.* **2022**, *580*, 152127. [[CrossRef](#)]
49. Gupta, M.K.; Bijwe, J.; Kadiyala, A.K. Tribo-Investigations on Oils with Dispersants and Hexagonal Boron Nitride Particles. *J. Tribol.* **2018**, *140*, 031801–031810. [[CrossRef](#)]
50. Ferrari, A.C.; Robertson, J. Interpretation of Raman Spectra of Disordered and Amorphous Carbon A. *Phys. Rev. B* **1969**, *31*, 632–645. [[CrossRef](#)]
51. Berman, D.; Erdemir, A.; Sumant, A.V. Few Layer Graphene to Reduce Wear and Friction on Sliding Steel Surfaces. *Carbon* **2013**, *54*, 454–459. [[CrossRef](#)]
52. Liñeira del Río, J.M.; López, E.R.; García, F.; Fernández, J. Tribological Synergies among Chemical-Modified Graphene Oxide Nanomaterials and a Phosphonium Ionic Liquid as Additives of a Biolubricant. *J. Mol. Liq.* **2021**, *336*, 116885. [[CrossRef](#)]
53. Kumar, N.; Saini, V.; Bijwe, J. Performance Properties of Lithium Greases with PTFE Particles as Additive: Controlling Parameter-Size or Shape? *Tribol. Int.* **2020**, *148*, 106302. [[CrossRef](#)]
54. Maurya, U.; Vasu, V. Boehmite Nanoparticles for Potential Enhancement of Tribological Performance of Lubricants. *Wear* **2022**, *498–499*, 204311. [[CrossRef](#)]
55. Srinivas, V.; Thakur, R.N.; Jain, A.K. Antiwear, Antifriction, and Extreme Pressure Properties of Motor Bike Engine Oil Dispersed with Molybdenum Disulfide Nanoparticles. *Tribol. Trans.* **2017**, *60*, 12–19. [[CrossRef](#)]